

A Hybrid Power Heronian Function-Based Multi-criteria Decision-making Model for Workplace Charging Scheduling Algorithms

Nuh Erdogan, *Member, IEEE*, Dragan Pamucar, Sadik Kucuksari, *Senior Member, IEEE* and Muhammet Deveci

Abstract—This study proposes a new multi-criteria decision-making model to determine the best smart charging scheduling that meets electric vehicle (EV) user considerations at workplaces. An optimal charging station model is incorporated into the decision-making for a quantitative evaluation. The proposed model is based on a hybrid Power Heronian functions in which the linear normalization method is improved by applying the inverse sorting algorithm for rational and objective decision-making. This enables EV users to specify and evaluate multi-criteria for considering their aspects at workplaces. Five different charging scheduling algorithms with AC dual port L2 and DC fast charging electric vehicle supply equipment (EVSE) are investigated. Based on EV users from the field, the required charging time, EVSE occupancy, the number of EVSE units, and user flexibility are found to have the highest importance degree, while charging cost has the lowest importance degree. The experimental results show that, in terms of meeting EV users' considerations at workplaces, scheduling EVs based on their charging energy needs performs better as compared to scheduling them by their arrival and departure times. While the scheduling alternatives display similar ranking behavior for both EVSE types, the best alternative may differ for the EVSE type. To validate the proposed model, a comparison against three traditional models is performed. It is demonstrated that the proposed model yields the same ranking order as the alternative approaches. Sensitivity analysis validates the best and worst scheduling alternatives.

Index Terms—EVSE, multi-criteria decision making, plug-in electric vehicles, smart charging scheduling, workplace charging.

I. INTRODUCTION

EXPANDING the charging infrastructure is crucial in transitioning to electric mobility [1]. Accordingly, the global number of chargers, also known as electric vehicle supply equipment (EVSE), continues to increase rapidly. The number of global private chargers has reached almost 10 million in 2020 with a total installed capacity of 55 GW [2]. Workplace EVSEs accommodate over 15 GW of the installed capacity. In this respect, workplace charging stations can play an important role in ensuring the smooth integration of electric vehicle (EV) charging loads into power systems. Thanks to their relatively longer dwell times and predictable

mobility, EVs at workplaces can provide ancillary services to the grid and aid in the integration of variable renewable energy sources for electricity generation [3]. However, smart charging strategies and scheduling are required to develop in order for EVs to provide such services.

For smooth EV grid integration (EVGI), smart charging has been the research focus for many recent studies [4]–[10]. Most studies formulate the EVGI as a single objective optimization problem, which is expressed using deterministic models such as linear, convex, or meta-heuristic [11]. The objective function can include several elements to represent technical and economic aspects such as charging costs, peak power, and so on from the perspective of the station owner, EV user, or utility [4]. In [5], a real-time controller is proposed to minimize the cost associated with EVGI at the workplace. For EV users, the cost is defined as the sum of charging and battery degradation costs. In [6], an optimal charging algorithm is implemented to minimize charging costs while adhering to the grid limits set by the utility. Moghaddam et al. [7], combine the objectives of minimizing EV travel distance, charging time, and charging cost with the weighted sum method to find the optimal option among EVSE types in an urban network, including battery swapping. Technical aspects such as energy losses, active and reactive loading of the transformer are included in the cost function for the EVGI in [8]. Furthermore, smart charging strategies are employed to help integrate renewable energy systems in distribution [9] and upstream networks [10]. In [9], a two-stage scheduling algorithm is proposed to reduce charging costs by increasing use of the photovoltaic system. The ancillary services provided by EVs to power systems such as congestion management, local voltage support, and spinning reserve are validated in a real distribution system in [12].

To maximize the benefits of smart charging, EVs can be scheduled both online and offline. For a given set of charging requests from EV users, scheduling EVs defines the order in which such requests are assigned to available EVSEs based on a heuristic assignment policy. Binetti et al. in [13] introduced several scheduling policies and evaluated their performance from a grid perspective. It was demonstrated that scheduling EVs by their charging flexibility with assigning the smallest slack time first performs the best grid performance. Ferguson et al. in [14] show that different scheduling methods result in different optimal workplace charging infrastructures, which affect the cost-benefit analysis. The use of smart charging for two scheduling algorithms was compared in [15]. When compared to sorting EVs based on their arrival times, sorting EVs by their flexibility resulted in improved peak reduction and increased cost savings as compared to sorting by their

N. Erdogan is with the School of Engineering, Robert Gordon University, Aberdeen AB10 7GJ, UK e-mail: (n.erdogan@rgu.ac.uk)

D. Pamucar, Department of Logistics, Military Academy, University of Defence in Belgrade, 11000 Belgrade, Serbia e-mail: (dpamucar@gmail.com)

S. Kucuksari is with the Department of Applied Engineering and Technical Management, University of Northern Iowa, Cedar Falls, IA, 50614 USA e-mail: (sadik.kucuksari@uni.edu)

M. Deveci is with Department of Industrial Engineering, Turkish Naval Academy, National Defence University, 34940, Istanbul, Turkey, and the Royal School of Mines, Imperial College London, SW7 2AZ, London, UK e-mail: (muhammetdeveci@gmail.com)

arrival times. In [16], a model predictive charging control is proposed to minimize charging costs based on clustering EVs by their state-of-charges (SOCs) and day-ahead market prices. Frendo et al. in [17] proposed a charging scheduling to maximize the fair use of the grid capacity among EVs based on their battery SOCs. The scheduling algorithms rely on the prediction of EVs' mobility. Liu et al. [18] introduced the urgency first charging policy. This policy ensures that the EVs with higher charging demand and shorter parking times are charged first. The charging urgency of EVs is calculated as the difference between the remaining time and the charging time estimation. Results show that the charging efficiency and charging convenience in terms of waiting and trip times have improved. Elghitani et al. [19] proposed a user-oriented method with a queueing model for the assignment of EVs to charging stations. It considers the average time spent by the EV user from requesting the charging service to accessing it as the performance indicator. The queueing model is used to facilitate the management of EV populations, and a Lyapunov optimization-based smart charging algorithm is then performed. Although the study focuses on queueing mainly after the request is received, it considers first-come, first-served scheduling for a dynamic population of EVs. A queueing network-based model is proposed in [20] for EV platoon charging processes in industrial transportation using renewable energy-aided charging stations. A contract theoretic approach for resource management is introduced for optimum charging policy. A Poisson process is assumed for EV platoon arrivals, and the EVs are served only based on a first-come-first-served policy. The proposed approach achieves optimal utility of the charging station with quality of service and regulates the peak demand on the grid. While these studies provide optimal solutions to the single objective problems expressed as the sum of several cost functions with technical constraints, EVGI can involve many objectives with technical, economic, and other social aspects that have been disregarded from an EV user perspective. As EV driving experience increases, many workplace considerations from EV users' perspectives such as EV user flexibility, charger occupancy time, and so on are becoming more prominent than charging cost. Therefore, there is a need to explore the best smart charging scheduling that meets all EV user considerations from a multi-criteria perspective.

Multi-objective problems have been regarded as multi-criteria decision-making (MCDM) problems which can involve both quantitative and qualitative parameters from various perspectives [21]–[23]. In these, various optimization algorithms can be included in the decision-making process. The MCDM method presents a selection framework for the best performing solution among optimal solutions, allowing the user to evaluate and weight multi-criteria decision-making variables into the decision [22]. As such, various MCDM models have been applied to many planning studies requiring critical decisions with potential technical, economic, and social consequences [21], [22], [24]. Liu et al. in [21] proposed a hybrid MCDM model by combining a grey decision-making trial and evaluation laboratory (DEMATEL) and uncertain linguistic multi-objective optimization by ratio analysis plus a full multiplicative form (UL-MULTIMOORA) for determining the most suitable public charging station location. In [22], an improved weighted aggregated sum product assessment-based MCDM

is proposed to select the best performing Pareto solution from a charging station owner perspective. Ma et al. in [23] utilize an MCDM scheme for selecting a voltage control solution that is supported by an evolutionary multi-objective optimization algorithm. In [24], the analytical hierarchy process (AHP) among MCDM methods is proposed to find the optimum parking slot in EV parking lots that weights the EV users' preferences. Tanaka et al. [25] apply the AHP method for substation maintenance and upgrade planning. Jiang et al. [26] investigated an MCDM approach for selecting the best access network in connected vehicle applications. In [27], a new MCDM method is proposed to determine the optimal combination of renewable sources for a microgrid. Some studies applied the Power or Heronian averaging operators to MCDM problems [28]–[31]. An interval-valued intuitionistic fuzzy Heronian mean operator is proposed in [28] for supplier selection in the supply chain. The generalized Heronian mean and geometric Heronian mean operators under the q-rung orthopair fuzzy sets are aggregated in [29] to evaluate the resource planning systems. Some operators are derived from the normal neutrosophic generalized weighted power averaging operator in [30]. Based on neutrosophic numbers, some aggregation operators are developed in [31] to solve multiple attribute group decision-making problems.

With the motivations stated above, this study proposes an improved MCDM model to determine the optimal EV scheduling at workplaces that perform the best from the EV user perspective. An optimal EVSE cost model is first developed from which EV user-related quantitative decision-making variables are calculated for various charging scheduling. The optimal model outputs are then integrated into the decision-making process. Using linguistic scores, the latter enables EV users to evaluate and weight the optimal decision-making variables. A new MCDM model is proposed by integrating Heronian averaging (HA) [32] and Power averaging (PA) [33] operators. The salient features of the proposed model can be highlighted as follows: (i) facilitating understanding of interactions between decision attributes, (ii) consideration is given to the interrelationships among the decision-making variables, (iii) the influence of extreme and unreasonable arguments in the initial matrix is eliminated, and (iv) taking into account the degree of support between the input arguments. In addition to these benefits of the hybrid Power Heronian function, the linear normalization technique is improved in this study by applying the inverse sorting algorithm [34]. The proposed approach for normalization of the cost attributed criteria defines two basic principles of normalization of multidimensional data: 1) preservation of the disposition of normalized values on the measurement scale and 2) absence of shifts in the areas of normalized values. Thus, a powerful MCDM tool for rational and objective evaluation of the performance of alternatives is obtained. To the best of the authors' knowledge, no research has considered the integration of hybrid Power Heronian functions and the inverse sorting algorithm into a single MCDM framework to date.

Five EV charging scheduling policies are defined as alternatives that can be implemented in workplaces. Using the optimal EVSE cost model, the performance of the scheduling policies are calculated for each decision-making variable considered. The decision-making variables are specified with the experts from the field based on EV user considerations at

workplaces. In terms of EVSE configuration, dual port AC L2 / Mode 3 at a charging rate of 22 kW and DC Fast Charging (DCFC) at 50 kW are considered. These EVSE types have gained popularity at workplaces [35]. According to a recent NREL report, the number of AC L2 and DCFC EVSE units for public and workplace charging stations is expected to increase by approximately 7 and 2 folds, respectively, by 2030. The hybrid Power Heronian function-based MCDM model is used to evaluate the performance of each scheduling alternative with the AC L2 and DCFC EVSE types. Hence, the best-performing scheduling from the EV user perspective is determined. The rest of this paper is organized as follows. In Section II, an optimal EVSE cost model for workplaces is developed and the solution to the model is discussed through smart charging scheduling. Section III presents the decision-making variables from the EV user perspective and the development of the hybrid MCDM model. Experimental results, including a sensitivity analysis, are presented and evaluated in Section IV. Finally, Section V provides concluding remarks.

II. AN OPTIMAL WORKPLACE CHARGING STATION MODEL WITH SMART CHARGING STRATEGY

A. Workplace Charging Behavior Model

The workplace EV charging characteristic has stochastic behavior that makes modeling challenging. Charging behaviour, such as charging energy and start time, may not be well represented by simple probability models such as the normal distribution. Some probability density functions (pdf) have been used to model charging behavior, including the kernel distribution [36]–[39], Gaussian Mixture Modeling (GMM) [40], [41], and Weibull distribution [42], [43]. The density estimation method can be different depending on the data set. In this study, the charging behavior at a business premise is modeled. The data was collected over a 6 month period from dual-port, AC L2 type (3-phase, 22 kW) EVSE units. To find the best representation, the data was modelled by the kernel distribution and GMM, and their characteristics were compared. For all charging behaviours (e.g., charging energy, charging start and end times), the goodness-of-fit of the kernel distribution is found to be superior to the GMM model. Based on the sample data, the kernel distribution is a non-parametric estimate of the pdf of the random variable [36]. Kernel density estimation can be formulated as:

$$f(x) = \frac{1}{nh} \sum_{i=1}^n K\left(\frac{x - x_i}{h}\right), \quad (1)$$

where x_1, x_2, \dots, x_n are random samples, n is the sample size, $K(\cdot)$ is the kernel smoothing function, and h is the bandwidth. In kernel estimation, the Gaussian (normal) kernel is commonly used [39] and formulated as:

$$K(x) = \frac{1}{\sqrt{2\pi}} e^{-x^2/2}. \quad (2)$$

The kernel bandwidth, h , needs to be optimized for the smoothness of the estimation. Matlab Statistics and Machine Learning Toolbox™ [44] is used to model the frequency distributions of charging energy, charging start and end times. Fig. 1 shows the histogram and kernel distribution of the charging start time of the collected data. These models are used to generate workplace charging behavior data for 100

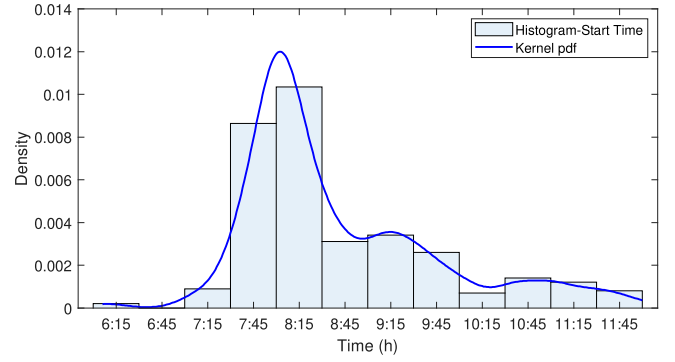


Fig. 1. Workplace EV charging start time and its Kernel distribution.

EVs to be used in the cost optimization model explained in Section II-B.

B. Cost Optimization Model for Workplace Charging Station

The EV charging procedure at the workplace EVSE can be formulated as an optimization problem whose objective is to minimize the daily levelized cost of charging [45]. The cost comprises three elements as follows: (i) daily charging energy cost, C_{op} , (ii) demand charge as a result of EV charging loads contributing to workplace peak demand, C_{dc} , (iii) daily levelized EVSE infrastructure cost, C_{LIC} , which includes EVSE unit hardware (C_{unit}), installation, and maintenance (C_{ins}) costs. Hence, the model can be constructed by a linear optimization problem as follows:

$$\min_{P_{ch,1} \dots P_{ch,n}, S_j} \left(C_{op}(P_{ch,i}) + C_{dc}(P_{ch,i}) + C_{LIC}(S_j) \right), \quad (3)$$

with,

$$C_{op} = \sum_{s_j=1}^{s_j} \sum_{i=1}^n \sum_{t=1}^T \left(F(t) \times (P_{ch,i,s_j}(t) \cdot \frac{\Delta t}{60}) \right), \quad (4)$$

$$C_{dc} = C_{dtrate} \cdot \left(\max \left(\sum_{k=1}^{96} \sum_{t=1}^{15} \text{mean} \left(\sum_{i=1}^{s_j} \sum_{j=1}^n P_{ch,i,s_j}((k-1) \cdot 15 + t) \right) \right) \right), \quad (5)$$

$$C_{LIC} = s_j \cdot AF \cdot (C_{unit} + C_{ins}), \quad (6)$$

subject to

$$\sum_{t=1}^T P_{ch,i}(t) \cdot \eta_i \cdot \frac{\Delta t}{60} = E_{required,i}, \quad (7)$$

$$\begin{cases} 0 \leq P_{ch,i}(t) \leq \min(\eta_i P_i^{rated}, \eta_j P_j^{rated}), & \text{if } L2 \\ 0 \leq P_{ch,i}(t) \leq \eta_j \cdot P_j^{rated}, & \text{if } DCFC \end{cases} \quad (8)$$

$$\sum_{t=1}^T \left(P_{base}(t) + \sum_{s_j=1}^{s_j} \sum_{i=1}^n P_{ch,i,s_j}(t) \right) \leq P_{lim}, \quad (9)$$

(3)-(6) minimize the daily levelized cost of charging with optimal charging rates while the EV user requirements are satisfied by constraint (7). (8) imposes EV charging rates in compliance with the standards IEC 61851/ SAE J1772s [11]. (9) ensures that the total power demand of the workplace, including the EV charging load, is always lower than the limit ($P_{lim} = 500$ kW) set in the tariff as a requirement for

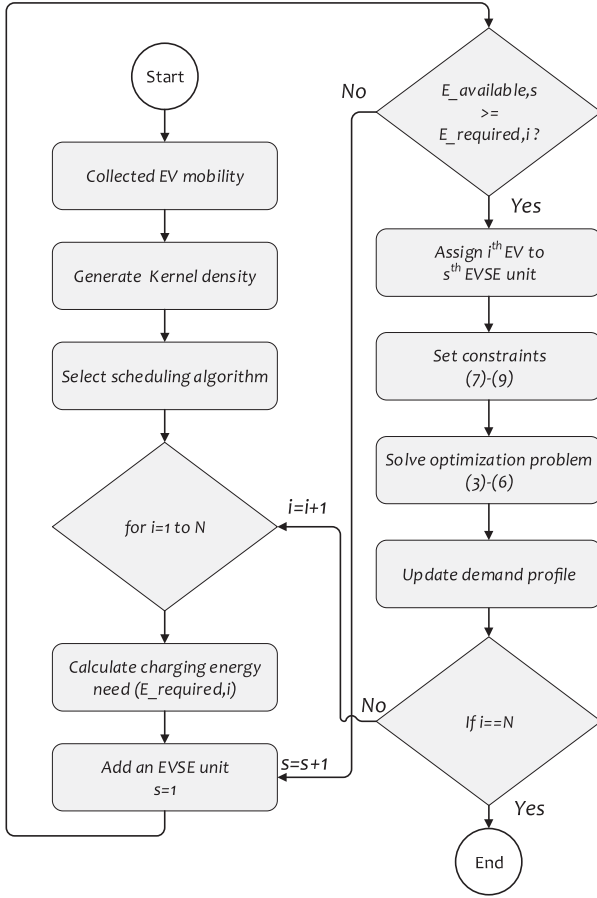


Fig. 2. Flow Chart of the smart charging algorithm.

medium power customers. $N = \{1, 2, \dots, n\}$ is set of EVs, $P_{ch,i} = \{P_{ch,i(1)} \dots P_{ch,i(T)}\}$ and $E_{required,i}$ are charging rates and energy need of the i^{th} EV, respectively. C_{drate} is the demand charge rate per kW. T is the number of time slots, $S = \{1, 2, \dots, s\}$ is the number of charging units. P_i^{rated} and η_i are the on-board charger power rating and its efficiency of i^{th} EV, respectively. P_j^{rated} and η_j are the power rating and the efficiency of the EVSE unit, respectively. P_{base} is the base load of the workplace in which the charging data is collected. $F = \{f(1) \dots f(T)\}$ is the daily energy cost offered by a utility company as a general demand time-of-use (ToU) tariff with three different rates [46]. To account for the time value of money, the annuity factor [47], AF , is set to 9.63% for a 5% discount rate and a 15-year lifetime of the EVSE units. The sum of C_{unit} and C_{ins} costs for AC L2 and DCFC are assumed to be 6,000 \$ and 58,000 \$, respectively.

A heuristic smart charging algorithm has been developed to solve the optimization problem (Fig. 2). Herein, the objective is set to maximize the use of EVSE units. As such, the number of EVSEs required is minimized. The proposed algorithm employs an interrupted charging profile [48] in which an EV is charged at optimum discrete time slots between its arrival and departure times. This charging scheme can be realized by an octopus type EVSE [15] in which only a single EV can be charged at a time while multiple EVs are connected to the EVSE. The algorithm assigns EVs to an EVSE sequentially based on the scheduling presented in the next subsection. When the EVSE can no longer accommodate

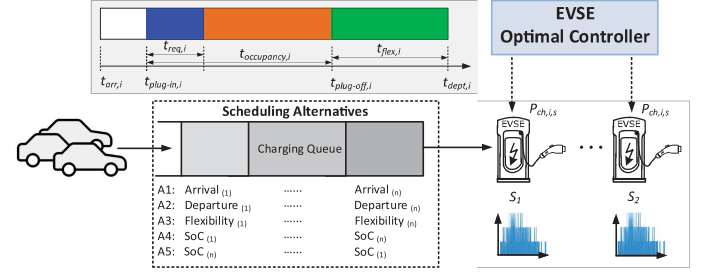


Fig. 3. The proposed framework of the integrated optimal workplace EVSE model with the charging scheduling for MCDM.

any EVs, an EVSE is added and the subsequent EVs continue to be assigned to the new EVSE until it cannot accommodate any EV. This algorithm is bidirectional in the sense that once a new EVSE is added, the previous EVSEs can also be used for subsequent EVs, which can be accommodated. This requires knowing the order in which EVs arrive. However, this is rational for a workplace charging station in which employees' mobility is more predictable. Furthermore, EV users are typically required to provide information about their mobility, such as daily commute, dwell times, and charging energy needs, in accordance with a policy developed by their employer.

C. Description of Charging Scheduling Alternatives

Because of their longer dwell times and predictable mobility patterns, EVs enable smart charging practices in the workplace. The smart charging algorithm involves decision-making about EV scheduling in order for both the charging station operator and the EV user to fully benefit from smart charging [49]. The proposed framework is illustrated in Fig. 3. It integrates the optimal EVSE model with an offline scheduling phase. While the smart charging algorithm determines optimal charging power rates in real-time for EVs at which optimal time slots and at which EVSE unit, the offline charging scheduling defines the order in which EVs have to be charged. This study addresses the practical applicability of scheduling at workplaces and therefore defines five scheduling policies as alternatives in ordering charging requests for a set of EVs. The two alternatives are based on time, while the three alternatives consider energy needs of EVs (e.g., their battery SOC).

The first alternative (A_1) is the first-come, first-served basis, which is the current charging practice at workplaces. The EVs are sorted based on their arrival times, and the EV with the earliest arrival time is assigned first by

$$A_1 = \underset{i \in \mathcal{N}}{\operatorname{argmin}} (t_{arr,i}), \quad (10)$$

where \mathcal{N} is the set of available EVs to schedule and $t_{arr,i}$ is the arrival time of i^{th} EV. The second alternative (A_2) is the earliest deadline first policy [13]. It sorts EVs based on their departure times and assigns the first EV with the earliest departure time as

$$A_2 = \underset{i \in \mathcal{N}}{\operatorname{argmin}} (t_{dept,i}), \quad (11)$$

where $t_{dept,i}$ is the departure time of i^{th} EV. The third alternative (A_3) sorts EVs by their flexibility ratios. It considers the ratio of dwell time to required charging time and sorts EVs

TABLE I
THE DECISION-MAKING VARIABLES.

Criterion Code	Criterion Name	Unit	Attribute Type
C1	Peak power	kW	Cost
C2	Energy charge	\$/kWh	Cost
C3	Demand charge	\$/kW	Cost
C4	EVSE cost	\$	Cost
C5	EVSE occupancy	%	Cost
C6	Required charging time	min	Cost
C7	Site factors	-	Cost
C8	Number of EVSE units	-	Benefit
C9	EVSE hosting capacity	%	Benefit
C10	User flexibility	%	Benefit

with respect to their flexibility ratios. The EV with the least flexibility is scheduled first by

$$A_3 = \underset{i \in \mathcal{N}}{\operatorname{argmin}} \left(\frac{t_{\text{dept},i} - t_{\text{arr},i}}{t_{\text{req},i}} \right), \quad (12)$$

where $t_{\text{req},i}$ is the required charging time of i^{th} EV. The fourth (A_4) and fifth (A_5) alternatives sort EVs according to their battery SOC levels. In (A_4), the EV with the highest required charging energy is scheduled first, while A_5 schedules the first EV with the lowest required charging energy as follows:

$$A_4 = \underset{i \in \mathcal{N}}{\operatorname{argmax}} (E_{\text{required},i}), \quad (13)$$

$$A_5 = \underset{i \in \mathcal{N}}{\operatorname{argmin}} (E_{\text{required},i}), \quad (14)$$

where $E_{\text{required},i}$ is the required charging energy of i^{th} EV.

III. DEVELOPMENT OF THE HYBRID POWER HERONIAN FUNCTION-BASED MCDM MODEL

A. Description of Decision-making Variables

Based on EV user considerations at workplaces from discussions with a workplace charging station operator and users in the field, this study specifies ten variables for a quantitative evaluation. As reported in Table I, the decision-making variables are attributed as either cost or benefit to allow the evaluation. Criteria weighting is not pre-supposed, but the degree of importance for each criterion is evaluated individually by the EV users from several workplaces. The EV driving experience of the users ranges from 1 year to 5 years.

The first variable is peak power, which is the commercial and industrial customers' highest electrical power demand (kW). When customers adopt large-scale EVs at workplaces, peak power has become one of the key considerations due to the higher peaks of their charging loads. Herein, $C1$, refers to the peak of the highest average charging power in 15-min intervals as in (5). From the optimization model run, the distribution of peak average charging demand for a group of 100 EVs for the charging schedulings considered is calculated for AC L2 and DCFC EVSEs as in Fig. 4 (a) and (b), respectively. It is shown that charging scheduling has a considerable effect on peak power. The lowest peak is achieved by the fourth alternative scheduling, while scheduling A_2 results in the highest peak. It is observed that scheduling by SOC level performs reduced peak power performance as compared to scheduling by arrival and departure times. While similar peak power behavior is observed when AC L2 EVSE is changed to DCFC, the lowest peak is achieved by A_4 in this case, as in Fig. 4 (b).

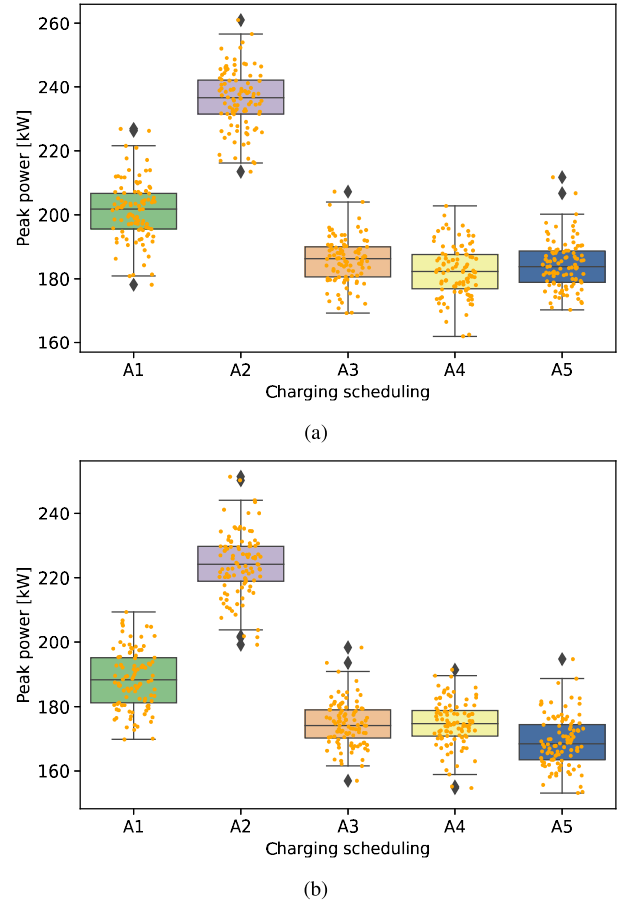


Fig. 4. Distribution of the decision-making variable $C1$ for 100 EVs with respect to the charging scheduling alternatives, (a) AC L2, (b) DCFC.

The next three variables form all the cost elements of charging at workplaces, which are considered in the objective function in (3). $C2$ is the energy charge, representing the daily electricity consumption cost to charge all EVs as in (4). $C3$ is the demand charge that covers the utility's cost for being able to meet the highest peak of average usage in 15 minutes, as in (5). $C4$ refers to the daily levelized EVSE cost, which covers the cost of unit hardware, installation, and maintenance over its life cycle as in (6). The demand charge and the EVSE cost are of interest to EV users since they might be reflected in the charging cost at workplaces. The distribution of $C2$, $C3$, and $C4$ for 100 EVs with AC L2 EVSE from the optimal model run is shown in Fig. 5. Scheduling by departure time achieves the lowest energy charge while they display the lowest performance in terms of demand charge and EVSE cost. Scheduling by SOC level demonstrates similar behavior and better performance for all cost elements as compared to scheduling by arrival time. In terms of deviations in cost figures, the scheduling type has the greatest impact on the demand charge. Similar behaviors are obtained for the DCFC EVSE type as well. Due to page limitations, the distributions for DCFC are not included in the paper. However, the average values over 100 random trials of the variables are reported in Table II.

EV users give a lot of consideration to the required charging time, $C6$, along with their dependency on being connected to the EVSE. While the required charging time is the time taken to achieve the desired SOC, EVSE occupancy, $C5$, is defined

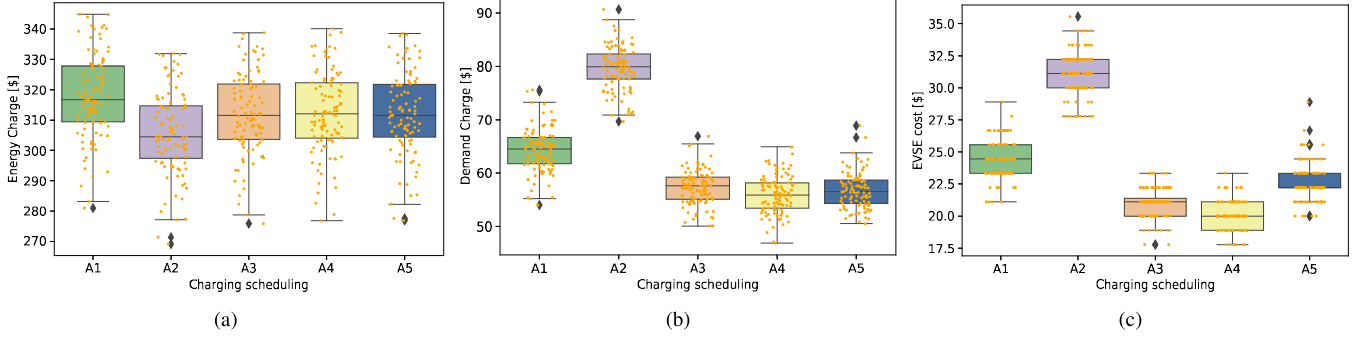


Fig. 5. Distribution of the decision-making variables with respect to AC L2 EVSE for 100 EVs with scheduling alternatives, (a) C_2 , (b) C_3 , (c) C_4 .

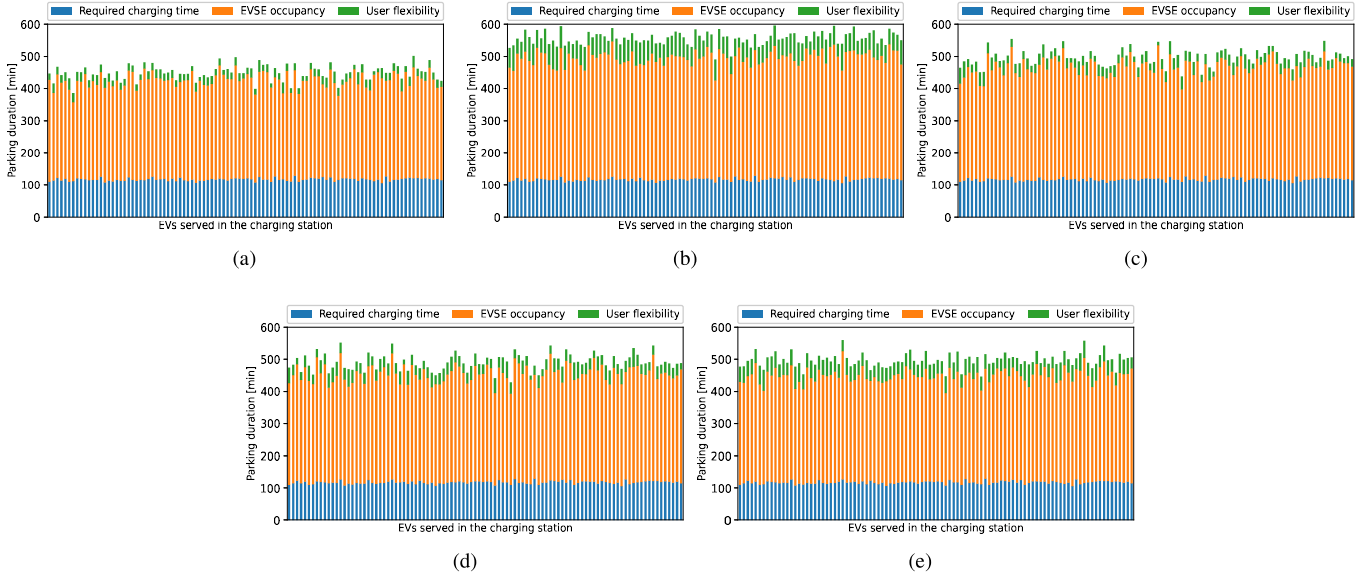


Fig. 6. Optimal results for the decision-making variables C_5 , C_6 , and C_{10} for 100 EVs with AC L2 with respect to charging scheduling: (a) A_1 , (b) A_2 , (c) A_3 , (d) A_4 , (e) A_5 . (Values are averaged over 100 random trials.)

by how much longer (%) an EV needs to remain connected to the EVSE unit than the required charging time. It is expressed as percentages by

$$EVSE_{ocp}(\%) = \text{mean}\left(\frac{t_{\text{plug-off},i} - t_{\text{plug-in},i}}{t_{\text{req},i}}\right) \cdot 100 \quad (15)$$

where $t_{\text{plug-in},i}$ and $t_{\text{plug-off},i}$ are the plug-in and plug off of i^{th} EV. In this respect, EV user flexibility, C_{10} , is defined as considering how sooner EV users can leave than their anticipated departure time with the desired SOC. Hence, it is expressed by

$$EV_{\text{flex}}(\%) = \text{mean}\left(\frac{t_{\text{deft},i} - t_{\text{plug-off},i}}{t_{\text{deft},i} - t_{\text{arr},i}}\right) \cdot 100 \quad (16)$$

The optimal model results for C_5 , C_6 , and C_{10} for a group of 100 EVs with the AC L2 option for the charging schedulings considered are shown in Fig. 6. While the percentages are used in calculations, for convenience, the time values of the occupancy C_5 and the user flexibility C_{10} as illustrated in Fig. 3 are shown in Fig. 6. The average required charging time is calculated to be 116 min, which is constant for all charging alternatives. To make use of off-peak times in the ToU tariff, the smart charging algorithm increases EVSE occupancy time

by more than three fold, which differs with respect to the charging alternatives. A_1 displays the best performance with the lowest average occupancy time of 309 minutes, while A_2 results in the highest occupancy time of 380 minutes. However, A_2 gives the most flexibility with an average time of 58 minutes. This is because, in the scheduling by departure time (A_2), the charging start times occur earlier. As such, the plug-off times with A_2 happen at an average of 20 minutes. In this respect, scheduling by SOC level displays similar EVSE occupancy performance with an average occupancy time of 340 minutes. Accordingly, they provide more flexibility by approximately 15 minutes with respect to A_1 . As the required charging time depends on the EVSE type rather than the scheduling algorithm, the average required charging time with DCFC EVSE is decreased by six fold with respect to the AC L2 type. In terms of EVSE occupancy and flexibility for the charging alternatives, a similar trend is obtained with DCFC EVSE as well. Due to page limitations, the figures for DCFC EVSE are not included in the paper.

In current practice, EVs usually need to be connected to EVSE units for longer than their required time. EV users can benefit from a higher number of EVSEs, C_8 , as it increases accessibility. However, the higher number of EVSE units can

be limited by various site factors, $C7$, including visibility and aesthetics. They may require electrical upgrades that will increase EVSE installation costs as well. Thus, the number of EVSE units at workplaces is considered as $C7$ and $C8$ variables from cost and benefit perspectives, respectively. The optimal values of the decision-making variables $C7$ and $C8$ for the charging alternatives are reported in Table II. In terms of EVSE unit number, for both EVSE types, A_2 requires the highest number of EVSE while the charging process is completed with the lowest EVSE numbers in A_4 . Another EV user consideration is EVSE hosting capacity (HC), $C9$. It is a measure of the efficient use of EVSE. While the AC EVSE power capacity is limited by the EVs whose onboard charger capacities are lower than that of the EVSE unit, $C9$ indicates how available time slots are efficiently used. It is expressed by

$$HC = \frac{\sum_i^n E_{required}(i)}{S_j(i) \cdot \frac{\max(tplug-off(1:n))}{\min(tplug-in(1:n))} \int (P_j^{rated} \cdot \eta_j) dt}. \quad (17)$$

The optimal HC values of the alternatives for dual-port AC L2 and DCFC EVSE are calculated as in Table II. The behavior of the alternatives displays similarities to both EVSE types. Scheduling by SOC level provides higher hosting capacity values as compared to scheduling by arrival or departure times. As such, A_4 was found to have the best hosting capacity with average values of 45.1% and 49.9%, while A_1 shows the lowest hosting capacity performance with average values of 30.5% and 32.6% for AC L2 and DCFC, respectively.

B. Preliminaries

The proposed MCDM model is based on the integration of HA and PA nonlinear functions. The definitions of weighted geometric HA and PA operators in the MCDM model are first given below. Then, the steps for implementing the proposed method are described.

Definition 1: [50]: Let $\phi, \varphi \geq 0$ and $(\partial_1, \partial_2, \dots, \partial_\chi)$ represent a set of non-negative numbers. The weighted Heronian operator (WHM) can be defined by

$$WHM^{\phi, \varphi}(\partial_1, \partial_2, \dots, \partial_\chi) = \frac{1}{\phi + \varphi} \left(\frac{2}{\chi(\chi + 1)} \sum_{x=1}^{\chi} (\chi w_x \partial_i^{(x)})^\phi \sum_{y=x}^{\chi} (\chi w_y \partial_j^{(y)})^\varphi \right)^{\frac{1}{\phi + \varphi}}. \quad (18)$$

Definition 2: [50]: Let $\phi, \varphi \geq 0$ and $(\partial_1, \partial_2, \dots, \partial_\chi)$ represent a set of non-negative numbers, then the weighted geometric Heronian operator (WGHM) can be defined by

$$WGHM^{\phi, \varphi}(\partial_1, \partial_2, \dots, \partial_\chi) = \frac{1}{\phi + \varphi} \left(\prod_{x=1, y=x}^{\chi} \left(\phi \partial_i^{(x) \chi w_i} + \varphi \partial_j^{(y) \chi w_j} \right)^{\frac{2}{\chi(\chi + 1)}} \right). \quad (19)$$

Definition 3: [33]: Let $(\partial_1, \partial_2, \dots, \partial_\chi)$ represent a set of non-negative numbers, the PA operator can be expressed by

$$PA(\partial_1, \partial_2, \dots, \partial_\chi) = \sum_{i=1}^{\chi} \partial_i \frac{\sum_{i=1}^{\chi} (1 + T(f(\partial_i))) f(\partial_i)}{\sum_{i=1}^{\chi} (1 + T(f(\partial_i)))}, \quad (20)$$

where $f(\partial_i) = \partial_i / \sum_{i=1}^{\chi} \partial_i$, while $T(f(\partial_i)) = \sum_{j=1, j \neq i}^{\chi} Sup(f(\partial_i), f(\partial_j))$ and $Sup(f(\partial_i), f(\partial_j))$ denotes the degree of support that ∂_i receives from ∂_j .

C. Hybrid Power Heronian Function-Based MCDM Framework

Suppose that the MCDM framework is defined to evaluate m alternatives represented by the set $A_i (i = 1, 2, \dots, m)$, through χ criteria denoted by $C_j (j = 1, 2, \dots, \chi)$. The steps for implementing the proposed hybrid MCDM are as follows:

Step 1. Form a home matrix. The home matrix elements $\aleph = [wp_{ij}]_{m \times \chi}$ are defined based on research into the characteristics of m alternatives in relation to the χ criteria, where wp_{ij} represents an estimate of the value of an i^{th} alternative in relation to the j^{th} criterion.

Step 2. Normalize the home matrix elements. Since the elements of the home matrix $\aleph = [\wp_{ij}]_{m \times \chi}$ are represented by different units of measurement, the elements \wp_{ij} are standardized by normalization, i.e., transformed into values that are in the interval $[0, 1]$. By applying (21), the normalized matrix is obtained. $\aleph^N = [\hat{\wp}_{ij}]_{m \times \chi}$.

$$\hat{\wp}_{ij} = \begin{cases} \hat{\wp}_{ij} = \frac{\wp_{ij}}{\wp_{ij}^+} & \text{if } j \in B \\ \hat{\wp}_{ij} = -\frac{\wp_{ij}}{\wp_{ij}^-} + \max\left(\frac{\wp_{ij}}{\wp_{ij}^+}\right) + \min\left(\frac{\wp_{ij}}{\wp_{ij}^-}\right) & \text{if } j \in C, \end{cases} \quad (21)$$

where $\wp_{ij}^+ = \max(\wp_{ij})$, $1 \leq i \leq m$, $1 \leq j \leq \chi$, B and C represent the benefit and cost attributes of criteria, respectively.

Step 3. Determine the weighting coefficients of the criteria. The weighting coefficients of the criteria are defined using a nonlinear model defined based on a full consistency comparison of the criteria according to the authors' previous study in [51], [52]. Experts $E = \{E_1, E_2, \dots, E_e\}$ evaluate the criteria using a predefined scale.

Step 3.1. Based on expert comparisons $\varpi_j^t (1 \leq t \leq e; j = 1, 2, \dots, \chi)$, the comparative significance of the criteria is determined. The value ϖ_j^t represents an expert assessment of the degree of importance for j^{th} criterion. Arithmetic averaging for each criterion yields a unique value $\varpi_j (j = 1, 2, \dots, \chi)$ which is used to define the vector of the comparative significance of criteria as follows:

$$\Omega = (\psi_1, \psi_2, \dots, \psi_\chi), \quad (22)$$

where the elements of the vector, Ω is obtained by applying the expression $\psi_j = \max(\varpi_j) / \varpi_j$, $1 \leq j \leq \chi$. Based on the vector of comparative significance, the ranking of the criteria is defined. As such, if the criterion has a higher value of ψ_j , then it is said to have greater significance and therefore have a better ranking.

Step 3.2. Calculate final values of weighting coefficients of criteria $w_j = (w_1, w_2, \dots, w_n)^T$. The final values of the coefficients should satisfy two groups of constraints, which are defined in the model (23).

$\min \varepsilon \text{ s.t.}$

$$\begin{aligned} & \left| \frac{w_j(k)}{w_j(k+1)} - \psi_{k+1} \right| \leq \varepsilon, \quad \forall j, \\ & \left| \frac{w_j(k)}{w_j(k+2)} - \psi_{k+1} \otimes \psi_{k+2} \right| \leq \varepsilon, \quad \forall j, \\ & \sum_{j=1}^{\chi} w_j = 1, w_j \geq 0, \quad \forall j, \end{aligned} \quad (23)$$

where k represents the ranking of the criterion defined based on the vector of the comparative significance of criteria.

Step 4. Calculate the significance of alternatives. Based on *Definitions 1, 2, and 3*, we define two hybrid functions for calculating the significance of alternatives as: (i) hybrid weighted Power Heronian function ($\mathbb{Q}_i^{(1),\phi,\varphi}$) and (ii) hybrid weighted geometric Power Heronian function ($\mathbb{Q}_i^{(2),\phi,\varphi}$), which are expressed by (24) and (25), respectively.

Theorem 1: Let $\hat{\phi}_{ij}(j = 1, 2, \dots, n)$ be a set of matrix elements $\mathbb{N}^N = [\hat{\phi}_{ij}]_{m \times \chi}$ and let $\phi, \varphi \geq 0$. If we denote the vector of weighting coefficients of the criteria by $w_j = (w_1, w_2, \dots, w_n)^T$, then the hybrid weighted averaging Power Heronian function, $\mathbb{Q}_i^{(1),\phi,\varphi}$, can be represented by

$$\begin{aligned} \mathbb{Q}_i^{(1),\phi,\varphi} = & \left(\frac{2}{\chi(\chi+1)} \sum_{x=1}^{\chi} \left(\chi \frac{n \hat{w}_i w_i}{\sum_{t=1}^n \hat{w}_t w_t} \hat{\phi}_i^{(x)} \right)^{\phi} \right. \\ & \left. \sum_{y=x}^{\chi} \left(\chi \frac{n \hat{w}_i w_j}{\sum_{t=1}^n \hat{w}_t w_t} \hat{\phi}_i^{(y)} \right)^{\varphi} \right)^{\frac{1}{\phi+\varphi}}. \end{aligned} \quad (24)$$

The proof for *Theorem 1* is provided in *Appendix A*.

Theorem 2: Let $\hat{\phi}_{ij}(j = 1, 2, \dots, n)$ be a set of matrix elements $\mathbb{N}^N = [\hat{\phi}_{ij}]_{m \times \chi}$ and let $\phi, \varphi \geq 0$. If we denote the vector of weighting coefficients of the criteria by $w_j = (w_1, w_2, \dots, w_n)^T$, then the hybrid weighted geometric Power Heronian function, $\mathbb{Q}_i^{(2),\phi,\varphi}$ can be represented by

$$\begin{aligned} \mathbb{Q}_i^{(2),\phi,\varphi} = & \frac{1}{\phi + \varphi} \left(\prod_{x=1, y=x}^{\chi} \left(\phi \hat{\phi}_i^{(x)} \chi \frac{n \hat{w}_i w_i}{\sum_{t=1}^n \hat{w}_t w_t} + \right. \right. \\ & \left. \left. \varphi \hat{\phi}_j^{(y)} \chi \frac{n \hat{w}_i w_j}{\sum_{t=1}^n \hat{w}_t w_t} \right)^{\frac{2}{\chi(\chi+1)}} \right). \end{aligned} \quad (25)$$

The proof for *Theorem 2* is provided in *Appendix A*.

Where in (24) and (25), $\hat{w}_t = \frac{(1+T(\hat{\phi}_i))}{\sum_{i=1}^{\chi} (1+T(\hat{\phi}_i))}$, while $T(\hat{\phi}_i) = \sum_{x=1, y \neq x}^{\chi} \text{Sup}(\hat{\phi}_i^{(x)}, \hat{\phi}_j^{(y)})$, $\sum_{i=1}^{\chi} \hat{w}_i = 1$, and $\text{Sup}(\hat{\phi}_i, \hat{\phi}_j)$ represents the degree of support that element $\hat{\phi}_i$ receives from element $\hat{\phi}_j$. Also, $\text{Sup}(\hat{\phi}_i, \hat{\phi}_j)$ satisfies the following three axioms:

- 1) $\text{Sup}(f(\hat{\phi}_i), f(\hat{\phi}_j)) = \text{Sup}(f(\hat{\phi}_j), f(\hat{\phi}_i))$
- 2) $\text{Sup}(f(\hat{\phi}_i), f(\hat{\phi}_j)) = [0, 1]$
- 3) $\text{Sup}(f(\hat{\phi}_i), f(\hat{\phi}_j)) > \text{Sup}(f(\hat{\phi}_i), f(\hat{\phi}))$, if $d(\hat{\phi}_i), d(\hat{\phi}_j) > d(\hat{\phi}_i), d(\hat{\phi})$, where $d(\hat{\phi}_i), d(\hat{\phi}_j)$ represents a distance between $\hat{\phi}_i$ and $\hat{\phi}_j$.

Step 5. Calculate the integrated value of the Power Heronian function as follow:

$$\mathbb{R}_i = \frac{\zeta \mathbb{Q}_1^{\phi,\varphi} + (1-\zeta) \mathbb{Q}_2^{\phi,\varphi}}{\sum_{i=1}^m (\zeta \mathbb{Q}_1^{\phi,\varphi} + (1-\zeta) \mathbb{Q}_2^{\phi,\varphi})}; \quad \zeta \in [0, 1] \quad (26)$$

TABLE II
HOME MATRICES.

Dual port AC L2 EVSE										
Alt.	C1	C2	C3	C4	C5	C6	C7	C8	C9	C10
A1	201.3	317.9	64.25	24.43	3.40	116.98	10.99	10.99	0.39	5.04
A2	236.0	305.8	79.62	31.11	4.61	116.98	14.00	14.00	0.31	11.11
A3	185.7	311.9	57.36	21.00	3.79	116.98	9.45	9.45	0.45	6.96
A4	182.4	312.3	55.93	20.03	3.62	116.98	9.02	9.02	0.47	8.17
A5	184.3	311.9	56.77	22.71	3.52	116.98	10.22	10.22	0.42	10.27
DCFC EVSE										
Alt.	C1	C2	C3	C4	C5	C6	C7	C8	C9	C10
A1	188.5	314.6	58.63	95.81	13.78	18.98	4.46	4.46	0.46	11.96
A2	224.2	300.6	74.39	131.04	23.70	18.98	6.10	6.10	0.33	19.39
A3	174.6	306.7	52.45	87.00	13.64	18.98	4.05	4.05	0.49	15.38
A4	174.8	306.5	52.54	85.50	12.75	18.98	3.98	3.98	0.49	17.63
A5	169.2	307.1	50.07	87.22	16.53	18.98	4.06	4.06	0.49	18.11

TABLE III
NORMALIZED MATRICES.

Dual port AC L2 EVSE										
Alt.	C1	C2	C3	C4	C5	C6	C7	C8	C9	C10
A1	0.920	0.962	0.895	0.859	1.000	1.0	0.859	0.785	0.824	0.454
A2	0.773	1.000	0.702	0.644	0.738	1.0	0.644	1.000	0.645	1.000
A3	0.986	0.981	0.982	0.969	0.916	1.0	0.969	0.675	0.954	0.627
A4	1.000	0.979	1.000	1.000	0.951	1.0	1.000	0.644	1.000	0.735
A5	0.992	0.981	0.989	0.914	0.974	1.0	0.914	0.730	0.883	0.924
DCFC EVSE										
Alt.	C1	C2	C3	C4	C5	C6	C7	C8	C9	C10
A1	0.914	0.956	0.885	0.921	0.957	1.0	0.921	0.731	0.912	0.617
A2	0.755	1.000	0.673	0.652	0.538	1.0	0.652	1.000	0.652	1.000
A3	0.976	0.981	0.968	0.989	0.962	1.0	0.989	0.664	0.985	0.794
A4	0.975	0.981	0.967	1.000	1.000	1.0	1.000	0.652	1.000	0.909
A5	1.000	0.979	1.000	0.987	0.840	1.0	0.987	0.666	0.981	0.934

Where ζ is the coefficient used to define the intensity of the influence of $\mathbb{Q}_1^{\phi,\varphi}$ and $\mathbb{Q}_2^{\phi,\varphi}$ functions on the final decision. As a general practice, a value of 0.5 was adapted. This ensures equal intensity of influence of both Power Heronian functions on the final decision.

Step 6. Finally, alternatives are ranked based on their values of \mathbb{R}_i . The higher \mathbb{R}_i , is, the better the alternative is.

IV. EXPERIMENTAL RESULTS

A. Results for Alternatives

The proposed MCDM methodology was applied to determine the best performing charging alternatives for two EVSE types, namely, dual-port AC L2 and DCFC. A set of five alternatives and ten criteria were formed within each EVSE type. The implementation of the methodology is presented as follows:

Step 1: In the first step, a home matrix was formed for each EVSE type, as in Table II where the values of the criteria were obtained from the optimal model run. The home matrices are defined for AC L2 and DCFC as follows: $\mathbb{N}^{L2MP} = [\hat{\phi}_{ij}]_{5 \times 10}$ and $\mathbb{N}^{DCFC} = [\hat{\phi}_{ij}]_{5 \times 10}$.

Step 2: Following forming the home matrix, the elements of the home matrices \mathbb{N}^{L2MP} and \mathbb{N}^{DCFC} were transformed into standardized values from the interval $\hat{\phi}_{ij} \in [0, 1]$ by using (21). Thus, the standardized values of home matrices were obtained as in Table III.

Step 3: The weighting coefficients of the criteria were defined by a group of EV users, $E = \{E_1, E_2, \dots, E_e\}$, from different workplaces. The experts evaluated the criteria as reported in Table IV using a nine-point scale: 1– Extremely Low, 2 – Medium Low, 3 – Low, 4 – Medium, 5 – Medium High, 6 – High, 7 – Very High, 8 – Extremely High, 9 – Perfect.

TABLE IV
EV USERS' EVALUATION OF CRITERIA.

Experts	Criteria									
	C1	C2	C3	C4	C5	C6	C7	C8	C9	C10
E1	8	4	5	7	4	5	5	5	5	7
E2	5	6	5	6	5	6	6	5	5	5
E3	1	5	3	6	9	9	7	9	7	6
E4	2	2	2	7	6	7	6	7	5	6
E5	6	6	7	4	6	6	6	6	6	6
E6	5	3	5	5	6	6	5	4	6	6
E7	7	5	8	5	8	8	8	7	5	7
Average	4.86	4.43	5.00	5.71	6.29	6.71	6.14	6.14	5.57	6.14

Step 3.1: Based on the EV users' evaluation in Table IV, using the expression $\psi_j = \max(\varpi_j)/\varpi_j$, the vector of the comparative significance of the criteria, (22), was formed by

$$\Omega = (0.0437, 0.0288, 0.0604, 0.0978, 0.1501, 0.1603, 0.1373, 0.1256, 0.0811, 0.1149)$$

The rank of criteria in Ω displays the significance of the criteria in which (C_6) was found to be the most important criterion while the least significant criterion was (C_2).

Step 3.2: The vector of final values of the weighting coefficients $w_j = (w_1, w_2, \dots, w_n)^T$ was calculated using the model given in (23).

$$\begin{aligned} \min \quad & \varepsilon \\ \text{s.t.} \quad & \left| \frac{w_6}{w_5} - 1.068 \right| \leq \varepsilon; \left| \frac{w_5}{w_7} - 1.093 \right| \leq \varepsilon; \left| \frac{w_7}{w_8} - 1.093 \right| \leq \varepsilon; \\ & \left| \frac{w_8}{w_{10}} - 1.093 \right| \leq \varepsilon; \\ & \left| \frac{w_{10}}{w_4} - 1.175 \right| \leq \varepsilon; \left| \frac{w_4}{w_9} - 1.205 \right| \leq \varepsilon; \left| \frac{w_9}{w_3} - 1.343 \right| \leq \varepsilon; \\ & \left| \frac{w_3}{w_1} - 1.382 \right| \leq \varepsilon; \\ & \left| \frac{w_1}{w_2} - 1.516 \right| \leq \varepsilon; \left| \frac{w_6}{w_7} - 1.168 \right| \leq \varepsilon; \left| \frac{w_5}{w_8} - 1.195 \right| \leq \varepsilon; \\ & \left| \frac{w_7}{w_{10}} - 1.195 \right| \leq \varepsilon; \\ & \left| \frac{w_8}{w_4} - 1.284 \right| \leq \varepsilon; \left| \frac{w_{10}}{w_9} - 1.416 \right| \leq \varepsilon; \left| \frac{w_4}{w_3} - 1.618 \right| \leq \varepsilon; \\ & \left| \frac{w_9}{w_1} - 1.856 \right| \leq \varepsilon; \\ & \left| \frac{w_3}{w_2} - 2.096 \right| \leq \varepsilon; \sum_{j=1}^{10} w_j = 1, w_j \geq 0, \quad \forall j. \end{aligned}$$

Lingo 19.0 software was used to solve the model, and the weighting coefficients of the criteria were obtained as follows: $w_1 = 0.0437, w_2 = 0.0288, w_3 = 0.0604, w_4 = 0.0978, w_5 = 0.1501, w_6 = 0.1603, w_7 = 0.1373, w_8 = 0.1256, w_9 = 0.0811, w_{10} = 0.1149$.

Step 4: Using (24) and (25) defines the significance of alternatives within AC L2 and DCFC as follows:

$$(i) \text{ for dual-port AC L2: } \mathbb{Q}_i^{(1)\phi=\varphi=1} = \begin{matrix} A_1 & 0.8496 \\ A_2 & 0.8322 \\ A_3 & 0.8884 \\ A_4 & 0.9147 \\ A_5 & 0.9270 \end{matrix};$$

$$\mathbb{Q}_i^{(2)\phi=\varphi=1} = \begin{matrix} A_1 & 0.8354 \\ A_2 & 0.8149 \\ A_3 & 0.8774 \\ A_4 & 0.9040 \\ A_5 & 0.9179 \end{matrix}$$

$$(ii) \text{ for DCFC: } \mathbb{Q}_i^{(1)\phi=\varphi=1} = \begin{matrix} A_1 & 0.8801 \\ A_2 & 0.8012 \\ A_3 & 0.9111 \\ A_4 & 0.9417 \\ A_5 & 0.9253 \end{matrix};$$

$$\mathbb{Q}_i^{(2)\phi=\varphi=1} = \begin{matrix} A_1 & 0.8687 \\ A_2 & 0.7840 \\ A_3 & 0.9010 \\ A_4 & 0.9316 \\ A_5 & 0.9163 \end{matrix}$$

For the calculation of the functions $\mathbb{Q}_i^{(1)\phi,\varphi}$ and $\mathbb{Q}_i^{(2)\phi,\varphi}$, the values of the parameters $\phi = \varphi = 1$ were adapted.

Step 5: The integrated values of the Power Heronian function of the alternatives with AC L2, \mathbb{R}_i^{L2MP} , and DCFC, \mathbb{R}_i^{DCFC} , were obtained by applying (26) as follows:

$$\mathbb{R}_i^{L2MP} = \begin{matrix} A_1 & 0.1923 \\ A_2 & 0.1880 \\ A_3 & 0.2015 \\ A_4 & 0.2076 \\ A_5 & 0.2106 \end{matrix}; \mathbb{R}_i^{DCFC} = \begin{matrix} A_1 & 0.1974 \\ A_2 & 0.1789 \\ A_3 & 0.2045 \\ A_4 & 0.2114 \\ A_5 & 0.2078 \end{matrix}$$

When calculating the integrated values of the alternatives by (26), the coefficient $\zeta = 0.5$ was adapted. This allows both functions $\left(\mathbb{Q}_i^{(1)\phi,\varphi} \text{ and } \mathbb{Q}_i^{(2)\phi,\varphi}\right)$ to have the same influence on the definition of the integrated values of the alternatives.

Step 6: The alternatives were ranked with respect to their integrated values, \mathbb{R}_i as follows: (i) for dual port AC L2; $A_5 > A_4 > A_3 > A_1 > A_2$, and (ii) for DCFC; $A_4 > A_5 > A_3 > A_1 > A_2$.

Regarding the EV users' ranking of criteria, the results in Table II reveal that required charging time, EVSE occupancy, number of EVSE units, and user flexibility were found to have the highest importance degree, while energy charge had the lowest importance degree. A_5 and A_4 were found to be the best performing charging alternatives for both AC L2 and DCFC EVSEs, while A_1 was the least feasible option for both EVSE types. While the optimal model yielded similar results for most of the criteria considered for A_4, A_5 , and A_3 with AC L2 EVSE, A_5 emerged as the most prominent option due to providing less EVSE occupancy and greater user flexibility. The primary reason for A_2 being the worst alternative is that it has the highest EVSE occupancy, the lowest hosting capacity, the highest demand charge, and the highest EVSE cost. It is observed that scheduling by SOC levels demonstrates superiority when considering all aspects of EV users at workplaces as their charging alternatives always remain in the top three. Similar behavior of the alternatives was observed for the DCFC unit as well. As being the best alternative, A_4 performs the lowest EVSE occupancy, number of EVSE units, demand charge, and highest hosting capacity. Similar to the performance with AC L2, scheduling by arrival and departure time with the DCFC unit displays the lowest performance for all aspects of EV users.

B. Sensitivity Analysis

In this section, the sensitivity analysis was performed to test the robustness of the obtained ranking solution. There are numerous approaches in the literature to analyze the robustness of MCDM models [52]–[56]. However, all approaches agree that robustness analysis depends on the specifics of the mathematical apparatus used in the MCDM model. Also, several authors [33], [57], [58] state that it is necessary to analyze the impact of subjectively defined input parameters on the initial results of the model. In the proposed MCDM framework, three parameters, ϕ, φ, ζ are defined based on the subjective preferences of experts. Subjectively defined parameters depend

on the conditions under which the system is modeled and the decision maker's perception. However, changing subjectively defined parameters can disrupt the stability of the initial solution. Therefore, it is recommended to perform a sensitivity and stability analysis of the solution. Sensitivity analysis is a simulation of the change of these parameters in the corresponding interval. Such an analysis enables the perception of the influence of subjective parameters on the final results of the model, i.e., it enables the verification of the stability of the initial results. Therefore, in this study, the strength of the initial solution depending on the variation of the parameters ϕ , φ , and ζ is analyzed.

a) *Influence of parameters ϕ and φ on the ranking results:* The expressions (24) and (25) show that the parameters, ϕ , φ , play an important role in defining the significance of alternatives and thus indirectly influence the final decision. An experiment was conducted by simulating the change of the parameters ϕ and φ in the interval $1 \leq \phi, \varphi \leq 50$. The effect of the ϕ and φ parameters on the change of values of the Power Heronian functions $Q_i^{(1)\phi, \varphi}$ and $Q_i^{(2)\phi, \varphi}$ for A_1 and A_2 alternatives is shown in Fig. 7. Similar changes happened in other alternatives within the two EVSE types considered.

The simulation was performed through 50 scenarios. In the first scenario, the value $\phi = \varphi = 1$ was adapted, while in each subsequent scenario, the value of parameters was increased by one. The results in Fig. 8 show that the change in parameter values significantly affects the values of the integrated function for the alternatives. It is observed that such changes can also shift the initial rank. An increase in the value of parameters within $1 \leq \phi, \varphi \leq 50$ decreases the integrated function scores of the top three ranked alternatives while increasing the integrated function scores of the last two ranked alternatives. Changing the parameters also reduces the difference in integrated function scores between alternatives A_1 , A_2 , A_3 , and A_4 shown in Fig. 8(a) and A_1 , A_3 , A_4 , and A_5 shown in Fig. 8(b). The values of the parameters $11 \leq \phi, \varphi \leq 16$, and $21 \leq \phi, \varphi \leq 50$ for AC L2 EVSE altered the rankings of the last three alternatives (A_1 , A_2 , and A_3). However, the rankings of the top two alternatives (A_5 and A_4) were confirmed. In order to analyze the statistical significance of these changes, the Spearman correlation coefficient (δ) was used. Using δ , a statistical correlation among rank changes was determined through 50 scenarios. Fig. 9 depicts the Spearman coefficient values.

The results show that the correlation ranges from $0.633 \leq \delta \leq 1$, which indicates a high correlation between the initial solution and the solutions in the scenarios. As a result of the analysis presented, it is possible to conclude that A_4 is the most dominant solution and that the initial ranking for the alternatives with the AC L2 EVSE unit is correct. The influence of varying parameters ϕ and φ on the values of the Power Heronian functions displays similar behavior for the alternatives to the DCFC EVSE. In this case, however, this does not change the rankings of alternatives as in Fig. 8(b). Therefore, this analysis can conclude that A_4 is the most dominant solution among the alternatives for the DCFC EVSE unit as well.

b) *Influence of parameter ζ on the ranking results* The ζ parameter was used to define the integrated values of the Power Heronian functions. In the initial calculation, the value of 0.5 was taken for ζ . The sensitivity analysis included 50

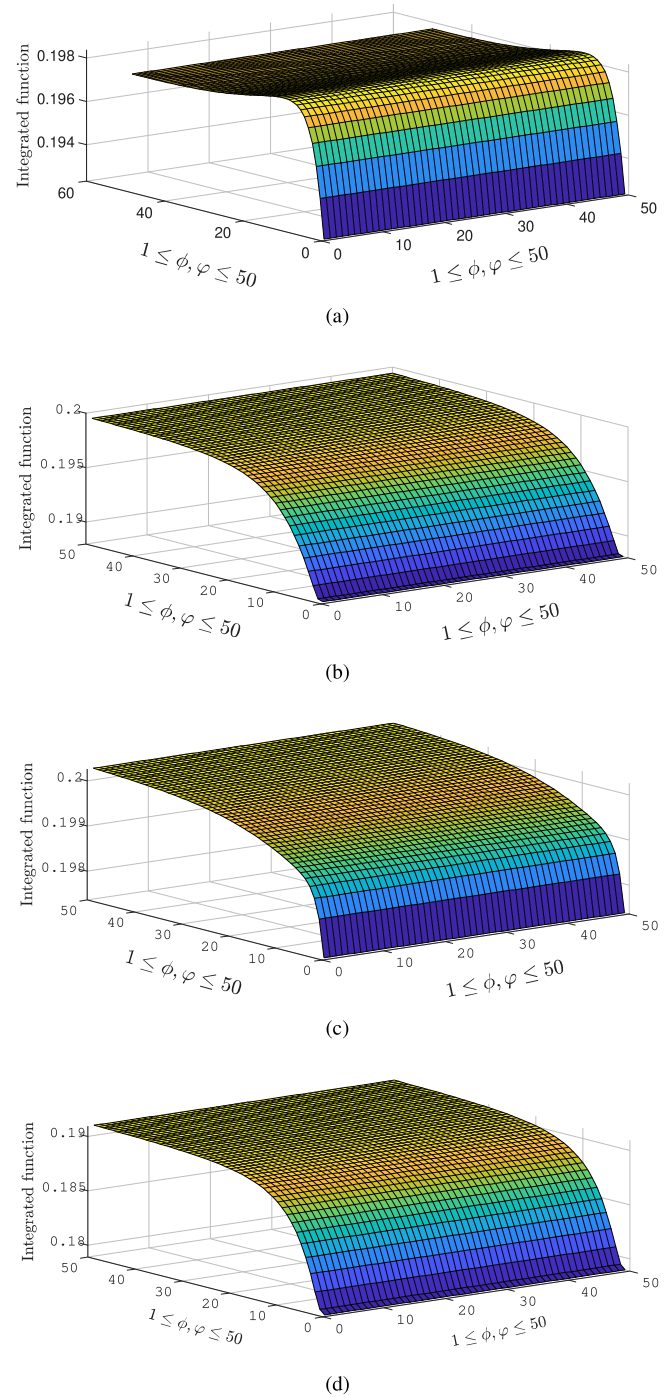


Fig. 7. Behavior of the integrated function scores with respect to varying parameters ϕ and φ for (a) A_1 with AC L2, (b) A_2 with AC L2, (c) A_1 with DCFC, and (d) A_2 with DCFC.

scenarios. The value $\zeta = 1.0$ was adapted in the first scenario, but in each subsequent scenario, the value of ζ was defined using the expression $\zeta^s = \zeta^{s-1} + 0.02$, where s represents the ordinal number of the scenario. The dependence of the integrated values of the alternatives with respect to varying ζ values is shown in Fig. 10. It is observed that changing ζ does not change the rankings of the alternatives for both EVSE types.

c) Comparative analysis

To test and validate the proposed MCDM model, it has been compared with traditional MCDM models. The MCDM

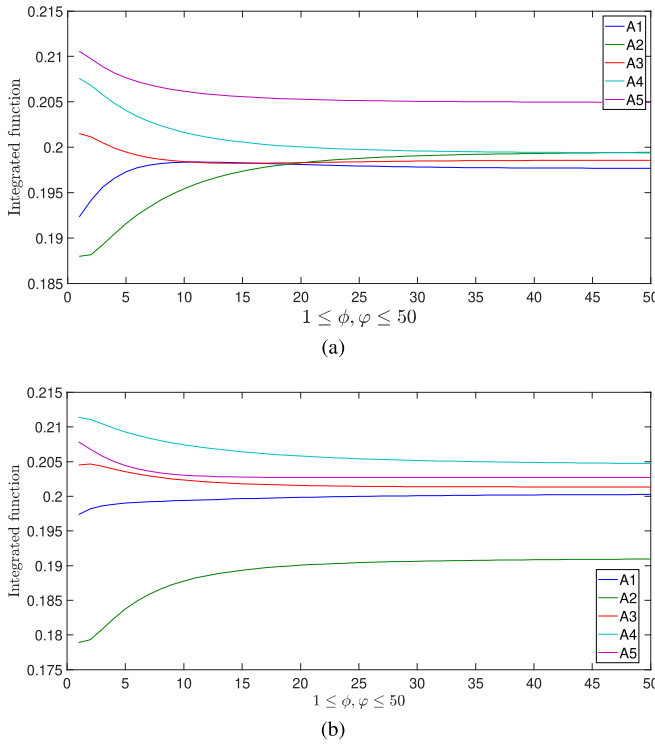


Fig. 8. Behavior of the integrated function scores of the alternatives with respect to varying parameters ϕ and φ , (a) L2MP, and (b) DCFC.

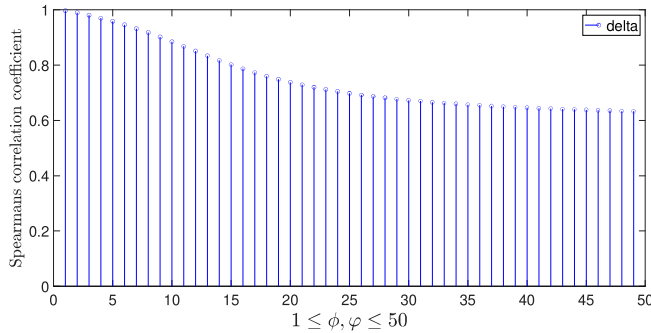


Fig. 9. Statistical correlation of the rankings.

methods that apply weighted linear functions for aggregation of information in the home matrix were selected for comparison. These are WASPAS (Weighted Aggregated Sum Product Assessment) method [59], RAFIS (Ranking of Alternatives through Functional mapping of criterion sub-intervals into a Single Interval) method [60] and VIKOR (VIekriterijumsko KOmpromisno Rangiranje) method [61]. After implementing these models, the ranking results are reported in Table V. In general, each MCDM model used yielded similar ranking results for each of the alternatives. The only difference found between the models is how the VIKOR approach ranked the alternatives A_3 and A_4 for AC L2 EVSE or A_5 for DCFC. This results from a consequence of applying a compromise pessimistic/optimistic index used to prioritize alternatives in the VIKOR method. However, all methods confirmed the credibility of the dominant alternatives, yielding the same best and worst alternatives. This indicates the robustness of the Power-Heronian functions methodology and the credibility of the proposed model. Table VI compares the features of the MCDM methods implemented along with the proposed model.

No restrictions are imposed on all MCDM methods used for

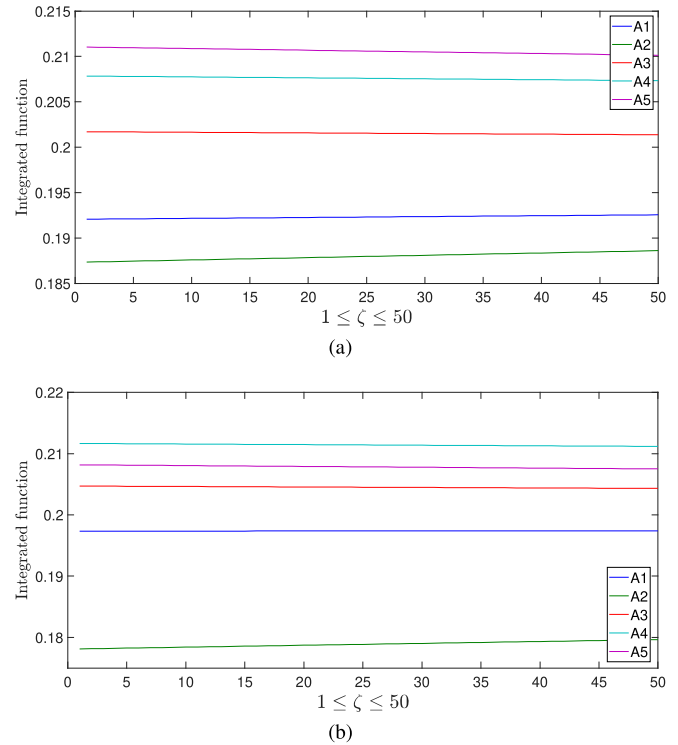


Fig. 10. Behavior of the integrated function scores of the alternatives with respect to varying parameter ζ values, (a) dual port AC L2, and (b) DCFC.

TABLE V
COMPARISON OF THE RANKINGS WITH VARIOUS MCDM METHODS.

	Dual port AC L2 EVSE					DCFC EVSE				
	A1	A2	A3	A4	A5	A1	A2	A3	A4	A5
Proposed	4	5	3	2	1	4	5	3	1	2
WASPAS	4	5	3	2	1	4	5	3	1	2
RAFIS	4	5	3	2	1	4	5	3	1	2
VIKOR	4	5	2	3	1	4	5	2	1	3

comparison regarding the number of alternatives or criteria. The choice of method depends on the conditions under which the decision is made. There are certain real-world situations in which decision-making requires considering the interrelationships between the criteria. In such situations, the advantages of the proposed model can be emphasized, which enables the recognition of mutual relations between the attributes and their fusion into a unique criterion function. Moreover, the aggregation functions in the traditional MCDM methods are linear, while hybrid nonlinear functions with stabilization parameters are used in the proposed model. The stabilization parameters of the proposed model enable flexible decision-making. As a result, the Power-Heronian methodology can be said to be more general and more flexible. In addition, one of the significant advantages of the proposed model is the elimination of extreme parameters from the home matrix. When the evaluation data has extreme values, the sorting results may be distorted with the traditional MCDM methods. However, the proposed method remains relatively stable in such situations because it can eliminate the influence of extreme values from prejudiced decision-makers based on power operators. Because of this characteristic, the proposed method may be used more broadly and is more suited for handling real-world decision-making problems. The inclusion of uncertainty theories into MCDM models complicates their mathematical formulation. The proposed method involves the

TABLE VI
THE COMPARISON OF THE MCDM METHODS IMPLEMENTED.

Methods	WASPAS [59]	RAFSI [60]	VIKOR [61]	Proposed
Features				
Allows the input parameters to support each other	No	No	No	Yes
Flexible decision-making due to decision makers' risk attitude	No	No	No	Yes
Flexibility in real-world applications	Partially	No	No	Yes
Eliminate the influence of extreme values from the decision matrix	No	No	No	Yes

iterative assessment of interactions between criteria, which further increases the mathematical complexity of the Power-Heronian approach if a request for processing complex information is made. However, the higher mathematical complexity of the proposed method has no effect on its overall efficiency and can be effectively eliminated by developing user-friendly software that significantly speeds up information processing.

V. CONCLUSION

In this study, a new MCDM model has been presented for selecting the best performing charging scheduling algorithm at workplaces from an EV user's multi-criteria perspective. The proposed model is based on integrating Power and Heronian averaging nonlinear functions, in which the linear normalization method is improved by applying the inverse sorting algorithm. For a quantitative evaluation, an optimal EVSE cost model was also incorporated into the decision-making. The model enabled EV users to specify and evaluate multi-criteria for considering their aspects at workplaces. Five different charging scheduling algorithms with AC dual port L2 and DCFC EVSE units have been studied.

EV users' considerations revealed that required charging time, EVSE occupancy, the number of EVSE units, and user flexibility were found to have the highest importance degree, while energy charge had the lowest importance degree. While the current literature has predominantly focused on minimizing charging costs, this study has shown that there are various parameters that should be taken into account rather than the charging cost. Considering ten quantitative criteria from different aspects of EV users at workplaces, the model found A_5 and A_4 as the best charging scheduling for AC L2 and DCFC, respectively, while A_2 displayed the lowest performance for both EVSE types. Moreover, the comparison analysis revealed a consistency among the results of the implemented MCDM models. The sensitivity analysis confirmed the validity of the best and worst alternatives. As a result, in terms of meeting EV users' considerations at workplaces, it was found that scheduling EVs by their charging energy needs (e.g.s SOC levels) performs better than scheduling by their arrival and departure times for both AC L2 and DCFC EVSE cases.

While the proposed MCDM model has yielded rational and objective evaluation performance, one of the limitations is the hybrid Power Heronian model's mathematical complexity. This feature might be a limiting factor in applying to other MCDM problems as well. Therefore, future work will be directed towards developing a user-oriented decision support system based on a rough Power Heronian methodology.

APPENDIX A

The proof of *Theorem 1*:

(18) is gradually decomposed into segments to derive (24). From (18) and (20), we can write that:

$$\chi w_i \hat{\phi}_i = \chi \sum_{t=1}^n \frac{n \hat{w}_i w_i}{\hat{w}_t w_t} \hat{\phi}_i ; \chi w_j \hat{\phi}_j = \chi \sum_{t=1}^n \frac{n \hat{w}_j w_j}{\hat{w}_t w_t} \hat{\phi}_j ;$$

Next, the multiplication of these two terms can be expressed by

$$\left(\chi w_i \hat{\phi}_i \right)^\phi \cdot \left(\chi w_j \hat{\phi}_j \right)^\varphi = \left(\chi \sum_{t=1}^n \frac{n \hat{w}_i w_i}{\hat{w}_t w_t} \hat{\phi}_i \right)^\phi \cdot \left(\chi \sum_{t=1}^n \frac{n \hat{w}_j w_j}{\hat{w}_t w_t} \hat{\phi}_j \right)^\varphi ,$$

that yields

$$\frac{2}{\chi(\chi+1)} \sum_{x=1, y=x}^{\chi} \left(\left(\chi w_i \hat{\phi}_i^{(x)} \right)^\phi \cdot \left(\chi w_j \hat{\phi}_j^{(y)} \right)^\varphi \right) = \frac{2}{\chi(\chi+1)} \sum_{x=1, y=x}^{\chi} \left(\left(\chi \sum_{t=1}^n \frac{n \hat{w}_i w_i}{\hat{w}_t w_t} \hat{\phi}_i^{(x)} \right)^\phi \cdot \left(\chi \sum_{t=1}^n \frac{n \hat{w}_j w_j}{\hat{w}_t w_t} \hat{\phi}_j^{(y)} \right)^\varphi \right) .$$

Finally, we get the function $Q_1^{\phi, \varphi}$ as follow:

$$Q_1^{\phi, \varphi} = \left(\frac{2}{\chi(\chi+1)} \sum_{x=1}^{\chi} \left(\chi \sum_{t=1}^n \frac{n \hat{w}_i w_i}{\hat{w}_t w_t} \hat{\phi}_i^{(x)} \right)^\phi \sum_{y=x}^{\chi} \left(\chi \sum_{t=1}^n \frac{n \hat{w}_j w_j}{\hat{w}_t w_t} \hat{\phi}_j^{(y)} \right)^\varphi \right)^{\frac{1}{\phi+\varphi}}$$

The proof of *Theorem 2*:

(19) is gradually decomposed into segments to derive (25).

From (19) and (20), we have

$$\phi \hat{\phi}_i^{\chi w_i} = \phi \hat{\phi}_i^{\sum_{t=1}^n \frac{\chi_i w_i}{\hat{w}_t w_t}} ; \varphi \hat{\phi}_j^{\chi w_j} = \varphi \hat{\phi}_j^{\sum_{t=1}^n \frac{\chi_j w_j}{\hat{w}_t w_t}}$$

Next, the summation of these two terms can be expressed by

$$\phi \hat{\phi}_i^{\chi w_i} + \varphi \hat{\phi}_j^{\chi w_j} = \left(\phi \hat{\phi}_i^{\sum_{t=1}^n \frac{\chi_i w_i}{\hat{w}_t w_t}} + \varphi \hat{\phi}_j^{\sum_{t=1}^n \frac{\chi_j w_j}{\hat{w}_t w_t}} \right),$$

that is expressed by

$$\prod_{x=1, y=x}^{\chi} \left(\phi \hat{\phi}_i^{\chi w_i} + \varphi \hat{\phi}_j^{\chi w_j} \right)^{\frac{2}{\chi(\chi+1)}} = \prod_{x=1, y=x}^{\chi} \left(\phi \hat{\phi}_i^{\sum_{t=1}^n \frac{\chi_i w_i}{\hat{w}_t w_t}} + \varphi \hat{\phi}_j^{\sum_{t=1}^n \frac{\chi_j w_j}{\hat{w}_t w_t}} \right)^{\frac{2}{\chi(\chi+1)}} .$$

Finally, we get the function $Q_2^{\phi, \varphi}$ as follow:

$$Q_2^{\phi, \varphi} = \frac{1}{\phi+\varphi} \left(\prod_{x=1, y=x}^{\chi} \left(\phi \hat{\phi}_i^{\chi w_i} \right)^{\chi \sum_{t=1}^n \frac{n \hat{w}_i w_i}{\hat{w}_t w_t}} + \varphi \hat{\phi}_j^{(y) \chi \sum_{t=1}^n \frac{n \hat{w}_j w_j}{\hat{w}_t w_t}} \right)^{\frac{2}{\chi(\chi+1)}}$$

ACKNOWLEDGMENT

The authors would like to thank EV users who participated in this study and Pat Mehigan for collecting charging data, sharing his experience with operating a workplace charging station, and his insightful suggestions.

REFERENCES

- [1] E. Ucer, I. Koyuncu, M. C. Kisacikoglu, M. Yavuz, A. Meintz, and C. Rames, "Modeling and analysis of a fast charging station and evaluation of service quality for electric vehicles," *IEEE Trans. Transport. Electrific.*, vol. 5, no. 1, pp. 215–225, 2019.
- [2] (2021) Global EV outlook: Accelerating ambitions despite the pandemic. <https://www.iea.org/reports/global-ev-outlook-2021>. [Online; accessed 01-Dec-2021].
- [3] N. Erdogan, S. Kucuksari, and U. Cali, "Co-simulation of optimal EVSE and techno-economic system design models for electrified fleets," *IEEE Access*, vol. 10, pp. 18 988–18 997, 2022.
- [4] R. Mehta, D. Srinivasan, A. M. Khambadkone, J. Yang, and A. Trivedi, "Smart charging strategies for optimal integration of plug-in electric vehicles within existing distribution system infrastructure," *IEEE Trans. Smart Grid*, vol. 9, no. 1, pp. 299–312, 2016.

- [5] V. Lakshminarayanan, V. G. S. Chemudupati, S. K. Pramanick, and K. Rajashekara, "Real-time optimal energy management controller for electric vehicle integration in workplace microgrid," *IEEE Trans. Transport. Electric.*, vol. 5, no. 1, pp. 174–185, 2018.
- [6] R. Aboalsleman and R. Scholer, "Smart charging: System design and implementation for interaction between plug-in electric vehicles and the power grid," *IEEE Trans. Transport. Electric.*, vol. 1, no. 1, pp. 18–25, 2015.
- [7] Z. Moghaddam, I. Ahmad, D. Habibi, and Q. V. Phung, "Smart charging strategy for electric vehicle charging stations," *IEEE Trans. Transport. Electric.*, vol. 4, no. 1, pp. 76–88, 2017.
- [8] S. S. K. Madahi, H. Nafisi, H. A. Abyaneh, and M. Marzband, "Co-optimization of energy losses and transformer operating costs based on smart charging algorithm for plug-in electric vehicle parking lots," *IEEE Trans. Transport. Electric.*, vol. 7, no. 2, pp. 527–541, 2020.
- [9] D. Wu, H. Zeng, C. Lu, and B. Boulet, "Two-stage energy management for office buildings with workplace ev charging and renewable energy," *IEEE Trans. Transport. Electric.*, vol. 3, no. 1, pp. 225–237, 2017.
- [10] H. N. Nguyen, C. Zhang, and J. Zhang, "Dynamic demand control of electric vehicles to support power grid with high penetration level of renewable energy," *IEEE Trans. Transport. Electric.*, vol. 2, no. 1, pp. 66–75, 2016.
- [11] M. Kisacikoglu, F. Erden, and N. Erdogan, "Distributed control of PEV charging based on energy demand forecast," *IEEE Trans. Ind. Informat.*, vol. 14, no. 1, pp. 332–341, Jan 2018.
- [12] K. Knezović, S. Martinenas, P. B. Andersen, A. Zecchino, and M. Marinelli, "Enhancing the role of electric vehicles in the power grid: field validation of multiple ancillary services," *IEEE Trans. Transport. Electric.*, vol. 3, no. 1, pp. 201–209, 2016.
- [13] G. Binetti, A. Davoudi, D. Naso, B. Turchiano, and F. L. Lewis, "Scalable real-time electric vehicles charging with discrete charging rates," *IEEE Trans. Smart Grid*, vol. 6, no. 5, pp. 2211–2220, Sept 2015.
- [14] B. Ferguson, V. Nagaraj, E. C. Kara, and M. Alizadeh, "Optimal planning of workplace electric vehicle charging infrastructure with smart charging opportunities," in *2018 21st Int. Conf. on Intelligent Transportation Systems (ITSC)*. IEEE, 2018, pp. 1149–1154.
- [15] E. R. Munoz and F. Jabbari, "A decentralized, non-iterative smart protocol for workplace charging of battery electric vehicles," *Applied Energy*, vol. 272, p. 115187, 2020.
- [16] K. Šepetanc and H. Pandžić, "A cluster-based model for charging a single-depot fleet of electric vehicles," *IEEE Trans. Smart Grid*, vol. 12, no. 4, pp. 3339–3351, 2021.
- [17] O. Frendo, N. Gaertner, and H. Stuckenschmidt, "Improving smart charging prioritization by predicting electric vehicle departure time," *IEEE Trans. Intell. Transp. Syst.*, vol. 22, no. 10, pp. 6646–6653, 2020.
- [18] S. Liu, Y. Cao, W. Ruan, Q. Ni, M. Nati, and C. Suthaputachakun, "Ev charging recommendation concerning preemptive service and charging urgency policy," in *2020 IEEE 92nd Vehicular Technology Conf. (VTC2020-Fall)*, 2020, pp. 1–5.
- [19] F. Elghitani and E. F. El-Saadany, "Efficient assignment of electric vehicles to charging stations," *IEEE Trans. Smart Grid*, vol. 12, no. 1, pp. 761–773, 2021.
- [20] K. Zhang, Y. Mao, S. Leng, Y. He, S. Maharjan, S. Gjessing, Y. Zhang, and D. H. K. Tsang, "Optimal charging schemes for electric vehicles in smart grid: A contract theoretic approach," *IEEE Trans. Intell. Transp. Syst.*, vol. 19, no. 9, pp. 3046–3058, 2018.
- [21] H.-C. Liu, M. Yang, M. Zhou, and G. Tian, "An integrated multi-criteria decision making approach to location planning of electric vehicle charging stations," *IEEE Trans. Intell. Transp. Syst.*, vol. 20, no. 1, pp. 362–373, 2018.
- [22] N. Erdogan, D. Pamucar, S. Kucuksari, and M. Deveci, "An integrated multi-objective optimization and multi-criteria decision-making model for optimal planning of workplace charging stations," *Applied Energy*, vol. 304, p. 117866, 2021.
- [23] H. Ma, K.-t. Ng, and K. F. Man, "A multiple criteria decision-making knowledge-based scheme for real-time power voltage control," *IEEE Trans. Ind. Informat.*, vol. 4, no. 1, pp. 58–66, 2008.
- [24] Z. Sadreddini, S. Guner, and O. Erdinc, "Design of a decision-based multi-criteria reservation system for the ev parking lot," *IEEE Trans. Transport. Electric.*, vol. 7, no. 4, pp. 2429–2438, 2021.
- [25] H. Tanaka, S. Tsukao, D. Yamashita, T. Niimura, and R. Yokoyama, "Multiple criteria assessment of substation conditions by pair-wise comparison of analytic hierarchy process," *IEEE Trans. Power Del.*, vol. 25, no. 4, pp. 3017–3023, 2010.
- [26] D. Jiang, L. Huo, Z. Lv, H. Song, and W. Qin, "A joint multi-criteria utility-based network selection approach for vehicle-to-infrastructure networking," *IEEE Trans. Intell. Transp. Syst.*, vol. 19, no. 10, pp. 3305–3319, 2018.
- [27] L. Zhang, F. Wang, Y. Xu, C.-H. Yeh, and P. Zhou, "Evaluating and selecting renewable energy sources for a microgrid: A bi-capacity-based multi-criteria decision making approach," *IEEE Trans. Smart Grid*, vol. 12, no. 2, pp. 921–931, 2020.
- [28] D. Yu and Y. Wu, "Interval-valued intuitionistic fuzzy heronian mean operators and their application in multi-criteria decision making," *African Journal of Business Management*, vol. 6, no. 11, pp. 4158–4168, 2012.
- [29] G. Wei, H. Gao, and Y. Wei, "Some q-rung orthopair fuzzy heronian mean operators in multiple attribute decision making," *Int. Journal of Intell. Syst.*, vol. 33, no. 7, pp. 1426–1458, 2018.
- [30] P. Liu and F. Teng, "Multiple attribute decision making method based on normal neutrosophic generalized weighted power averaging operator," *Int. Journal of Machine Learning and Cybernetics*, vol. 9, no. 2, pp. 281–293, 2018.
- [31] P. Liu and X. Liu, "The neutrosophic number generalized weighted power averaging operator and its application in multiple attribute group decision making," *Int. Journal of Machine Learning and Cybernetics*, vol. 9, no. 2, pp. 347–358, 2018.
- [32] D. Yu, "Intuitionistic fuzzy geometric heronian mean aggregation operators," *Applied Soft Computing*, vol. 13, no. 2, pp. 1235–1246, 2013.
- [33] R. R. Yager, "The power average operator," *IEEE Trans. Syst., Man, Cybern. A, Syst. Humans*, vol. 31, no. 6, pp. 724–731, 2001.
- [34] I. Z. Mukhametzyanov, "Res-algorithm for converting normalized values of cost criteria into benefit criteria in medm tasks," *Int. Journal of Information Technology & Decision Making*, vol. 19, no. 05, pp. 1389–1423, 2020.
- [35] A. Brown, A. Schayowitz, and E. Klotz, "Electric Vehicle Charging Infrastructure Trends from the Alternative Fueling Station Locator: First Quarter 2021," Tech. Rep. NREL/TP-5400-80684, 1820581, MainId:77468, Sep. 2021. [Online]. Available: <https://www.osti.gov/servlets/purl/1820581>
- [36] N. G. Paterakis and M. Gibescu, "A methodology to generate power profiles of electric vehicle parking lots under different operational strategies," *Applied Energy*, vol. 173, pp. 111–123, Jul. 2016.
- [37] S. Schaeck, T. Karspeck, C. Ott, M. Weckler, and A. Stoermer, "A field operational test on valve-regulated lead-acid absorbent-glass-mat batteries in micro-hybrid electric vehicles. Part I. Results based on kernel density estimation," *Journal of Power Sources*, vol. 196, no. 5, pp. 2924–2932, Mar. 2011.
- [38] C. Ran, Y. Zhang, and Y. Yin, "Demand response to improve the shared electric vehicle planning: Managerial insights, sustainable benefits," *Applied Energy*, vol. 292, p. 116823, Jun. 2021.
- [39] M. Liang, W. Li, J. Yu, and L. Shi, "Kernel-based electric vehicle charging load modeling with improved latin hypercube sampling," in *2015 IEEE Power & Energy Society General Meeting*. Denver, CO, USA: IEEE, Jul. 2015, pp. 1–5.
- [40] J. Quirós-Tortós, A. Navarro-Espinosa, L. F. Ochoa, and T. Butler, "Statistical representation of ev charging: Real data analysis and applications," in *2018 Power Systems Computation Conf. (PSCC)*. IEEE, 2018, pp. 1–7.
- [41] S. Torres, I. Durán, A. Marulanda, A. Pavas, and J. Quirós-Tortós, "Electric vehicles and power quality in low voltage networks: Real data analysis and modeling," *Applied Energy*, vol. 305, p. 117718, Jan. 2022.
- [42] J. Zhang, J. Yan, Y. Liu, H. Zhang, and G. Lv, "Daily electric vehicle charging load profiles considering demographics of vehicle users," *Applied Energy*, vol. 274, p. 115063, Sep. 2020.
- [43] Y. B. Khoo, C.-H. Wang, P. Paevere, and A. Higgins, "Statistical modeling of Electric Vehicle electricity consumption in the Victorian EV Trial, Australia," *Transportation Research Part D: Transport and Environment*, vol. 32, pp. 263–277, Oct. 2014.
- [44] Matlab. (R2021b) Statistics and machine learning toolbox. [Online]. Available: <https://www.mathworks.com/products/statistics.html>
- [45] N. Erdogan, S. Kucuksari, and J. Murphy, "A multi-objective optimization model for evse deployment at workplaces with smart charging strategies and scheduling policies," *Energy*, p. 124161, 2022.
- [46] P. Gas and E. Company. (July 8, 2021) Medium general demand-metered service. [Online]. Available: <https://www.pge.com/tariffs/index.page>
- [47] A. Schroeder and T. Traber, "The economics of fast charging infrastructure for electric vehicles," *Energy Policy*, vol. 43, pp. 136–144, 2012.
- [48] A. Malhotra, N. Erdogan, G. Binetti, I. D. Schizas, and A. Davoudi, "Impact of charging interruptions in coordinated electric vehicle charging," in *Signal and Information Processing (GlobalSIP), 2016 IEEE Global Conf.* IEEE, 2016, pp. 901–905.
- [49] O. Frendo, N. Gaertner, and H. Stuckenschmidt, "Real-time smart charging based on precomputed schedules," *IEEE Trans. Smart Grid*, vol. 10, no. 6, pp. 6921–6932, 2019.
- [50] S. Zhao, D. Wang, C. Liang, Y. Leng, and J. Xu, "Some single-valued neutrosophic power heronian aggregation operators and their application to multiple-attribute group decision-making," *Symmetry*, vol. 11, no. 5, p. 653, 2019.

- [51] D. Pamučar, Ž. Stević, and S. Sremac, "A new model for determining weight coefficients of criteria in mcdm models: Full consistency method (fucom)," *Symmetry*, vol. 10, no. 9, p. 393, 2018.
- [52] D. Pamucar and F. Ecer, "Prioritizing the weights of the evaluation criteria under fuzziness: The fuzzy full consistency method—fucom-f," *Facta Universitatis, Series: Mechanical Engineering*, vol. 18, no. 3, pp. 419–437, 2020.
- [53] S. Zolfani, M. Yazdani, D. Pamucar, and P. Zarate, "A vikor and topsis focused reanalysis of the madm methods based on logarithmic normalization," *arXiv preprint arXiv:2006.08150*, 2020.
- [54] Z. Ali, T. Mahmood, K. Ullah, and Q. Khan, "Einstein geometric aggregation operators using a novel complex interval-valued pythagorean fuzzy setting with application in green supplier chain management," *Reports in Mechanical Engineering*, vol. 2, no. 1, pp. 105–134, 2021.
- [55] D. Pamučar, M. Žižović, S. Biswas, and D. Božanić, "A new logarithm methodology of additive weights (lmaw) for multi-criteria decision-making: Application in logistics," *Facta Universitatis, Series: Mechanical Engineering*, 2021.
- [56] D. Bozanic, D. Tešić, and A. Milić, "Multicriteria decision making model with z-numbers based on fucom and mabac model," *Decision Making: Applications in Management and Engineering*, vol. 3, no. 2, pp. 19–36, 2020.
- [57] F. Sinani, Z. Erceg, and M. Vasiljević, "An evaluation of a third-party logistics provider: The application of the rough dombi-hamy mean operator," *Decision Making: Applications in Management and Engineering*, vol. 3, no. 1, pp. 92–107, 2020.
- [58] L. Muhammad, I. Badi, A. A. Haruna, and I. Mohammed, "Selecting the best municipal solid waste management techniques in nigeria using multi criteria decision making techniques," *Reports in Mechanical Engineering*, vol. 2, no. 1, pp. 180–189, 2021.
- [59] E. K. Zavadskas, Z. Turskis, J. Antucheviciene, and A. Zakarevicius, "Optimization of weighted aggregated sum product assessment," *Elektronika ir elektrotechnika*, vol. 122, no. 6, pp. 3–6, 2012.
- [60] M. Žižović, D. Pamučar, M. Albijanić, P. Chatterjee, and I. Pribičević, "Eliminating rank reversal problem using a new multi-attribute model—the rafsi method," *Mathematics*, vol. 8, no. 6, p. 1015, 2020.
- [61] S. Opricovic and G.-H. Tzeng, "Compromise solution by mcdm methods: A comparative analysis of vikor and topsis," *European journal of operational research*, vol. 156, no. 2, pp. 445–455, 2004.



Nuh Erdogan received the Ph.D. degree in electrical engineering from the University of Picardie Jules Verne, Amiens, France, in 2006. He is a fellow of the UK Higher Education Academy and is currently an Assistant Professor in the School of Engineering at Robert Gordon University (RGU). Prior to joining RGU, he was with the Marine and Renewable Energy Centre of Ireland as a Research Fellow between 2018–2021 and with the University of Texas at Arlington as a visiting Research Scholar between 2016–2018. In addition

to these, he had an R&D Program development, implementation, and project management experience in the research funding agency of Turkey. His research interests include the electricity grid integration of renewable energy technologies and plug-in electric vehicles. He was the recipient of several international awards and grants, including the best paper award in Modern Power Systems and Clean Energy, the International Post-Doctoral Fellowship Award, and the International PhD scholarship award.



Dr. Dragan Pamucar is an Associate Professor at the University of Belgrade, Faculty of Organizational Sciences, Serbia. He received a PhD in Applied Mathematics with a specialization in Multi-criteria modeling and soft computing techniques from the University of Defence in Belgrade, Serbia in 2013 and an MSc degree from the Faculty of Transport and Traffic Engineering in Belgrade in 2009. His research interests are in the fields of computational intelligence, multi-criteria decision making problems, neuro-fuzzy systems, fuzzy, rough, and intuitionistic fuzzy set theory, and neutrosophic theory. Application areas include a wide range of logistics problems. He has five books and over 200 research papers published in international journals, including Expert Systems with Applications, Applied Soft Computing, Soft Computing, Information Sciences, Computational Intelligence, Computers, and Industrial Engineering. He has been awarded the top and outstanding reviewer for numerous journals. According to Scopus and Stanford University, he is among the world's top 2% of scientists as of 2020.



the electrical power grid, plug-in electrical vehicles, distribution and transmission of electrical power.

Dr. Sadik Kucuksari (M'11, SM'22) received a Ph.D. degree in electrical engineering from Arizona State University, Tempe, AZ, in 2010. He is currently an Associate Professor in the Dept. of Applied Engineering and Technical Management at University of Northern Iowa. Prior to joining UNI, he was an Assistant Professor at Alabama A&M University between 2012–2014. He was a postdoctoral scholar at University of Arizona between 2010–2012. His research interests include integration of renewable energy sources with



Dr. Muhammet Deveci is currently a Visiting Professor at the Royal School of Mines at Imperial College London, UK, and he is an Honorary Senior Research Fellow with the Barlett School of Sustainable Construction, University College London, UK. He is also an Associate Professor at the Department of Industrial Engineering at the Turkish Naval Academy and National Defence University, Istanbul, Turkey. He worked as a Visiting Researcher and Postdoctoral Researcher, in 2014–2015 and 2018–2019, respectively, with the School of Computer Science, University of Nottingham, Nottingham, U.K. He has published over 70 papers in international journals and over 23 contributions at international conferences. He has been a member of editorial boards and worked as a guest editor for several international journals, such as IEEE Transactions on Fuzzy Systems, Applied Soft Computing, Sustainable Energy Technologies and Assessments, the Journal of Petroleum Science and Engineering, and the International Journal of Hydrogen Energy. His research focuses on computational intelligence, uncertainty handling, fuzzy sets and systems, fuzzy decision making, decision support systems, modeling and optimization applied to complex real-world problems including climate change, renewable energy, sustainable transportation, humanoid robots, autonomous vehicles, digitalization, and the circular economy.